World Academy of Science, Engineering and Technology
International Journal of Urban and Civil Engineering
Vol:14, No:4, 2020

Sedimentary Response to Coastal Defense Works in São Vicente Bay, São Paulo

L. C. Ansanelli, P. Alfredini

***Abstract*—**The article presents the evaluation of the effectiveness of two groins located at Gonzaguinha and Milionários Beaches, situated on the southeast coast of Brazil. The effectiveness of these coastal defense structures is evaluated in terms of sedimentary dynamics, which is one of the most important environmental processes to be assessed in coastal engineering studies. The applied method is based on the implementation of the Delft3D numerical model system tools. Delft3D-WAVE module was used for waves modelling, Delft3D-FLOW for hydrodynamic modelling and Delft3D-SED for sediment transport modelling. The calibration of the models was carried out in a way that the simulations adequately represent the region studied, evaluating improvements in the model elements with the use of statistical comparisons of similarity between the results and waves, currents and tides data recorded in the study area. Analysis of the maximum wave heights was carried to select the months with higher accumulated energy to implement these conditions in the engineering scenarios. The engineering studies were performed for two scenarios: 1) numerical simulation of the area considering only the two existing groins; 2) conception of breakwaters coupled at the ends of the existing groins, resulting in two "T" shaped structures. The sediment model showed that, for the simulated period, the area is affected by erosive processes and that the existing groins have little effectiveness in defending the coast in question. The implemented T structures showed some effectiveness in protecting the beaches against erosion and provided the recovery of the portion directly covered by it on the Milionários Beach. In order to complement this study, it is suggested the conception of further engineering scenarios that might recover other areas of the studied region.

***Keywords*—**Coastal engineering, coastal erosion, Sao Vicente Bay, Delft3D, coastal engineering works.

I. Introduction

THE movement of sedimentary particles on the coast under the influence of tide, winds and wind-driven waves is a complex and intriguing problem. The combination of field observations, laboratory experiments and theoretical development is key to elaborate scientific knowledge and engineering solutions for sedimentary problems in coastal regions, yet it is a complex task [1].

In recent years, a wide range of research based on laboratory experiments and field observations have sought to measure the transport processes induced by waves and currents and, as a result, some predictive approaches have been developed [1]. Generally, these approaches can be divided into two classes: (1) processes based on numerical models and (2) parameterized formulations.

Approaches based on numerical models represent many physical processes involved in the transport of sediments by waves and currents and solve the vertical and even horizontal structure of non-stationary wave propagation velocities and concentration of sedimentary particles. Coastal morphodynamic model systems (e.g. Delft3D, Telemac and Mike) solve wave-generated fluxes, diffusion and advection equations to determine temporal averages in the suspended sediment concentration field [1].

Erosive processes in coastal regions have been observed and studied all over the world with different methodologies and are described in technical literature. In the scope of coastal engineering in Brazil, an important challenge is the elaboration of mitigation plans as a response to the impacts in the coastline that are related to anthropic intervention and climate-driven processes. The coast of the São Paulo state in Southeast Brazil frequently shows this type of erosion process at several spatial and temporal scales due to the combination of the dynamics of the internal continental platform systems and the coastline orientation [2].

The Baixada Santista (Fig. 1), in the coastal region of the São Paulo state, has been experiencing problems with storm surges reaching the entire coast. The São Vicente Bay, located at the Baixada Santista, is confined between the São Vicente and Porchat islands and Ponta do Itaipu located in the mainland. Its exit is towards SE and is protected by rock outcrops. The coastline at São Vicente Bay is oriented approximately NW-SE at Milionários Beach and E-W at Gonzaguinha Beach (Fig. 1).

The establishment of a permanent connection between the São Vicente (Milionários Beach) and Porchat Island by artificial landfills in the 1950s interrupted the sand transportation by drift currents from the marine areas to the interior of the São Vicente Bay. This fact is considered as the triggering factor of the beach erosion processes observed today, as a result of the interruption of hydrodynamic mechanisms (i.e. currents generated by waves), that transferred sand from Santos Bay to the interior of São Vicente Bay [3].

The interrupted source of sand described above and the absence of significant alternative sources of granular material, combined with the incidence of waves in the internal areas of the system results in the remobilization of the sand from the beaches to the deeper regions of the Bay. The erosive process was already significant in the 1950s and led the public authorities to build the groins as an attempt to attenuate the erosive processes and reduce the direct impact of wave

L. C. Ansanelli is with the Polytechnic School of Universidade de São Paulo, São Paulo, SP 05508-010 Brazil (corresponding author, phone: 014-9771-1812; e-mail: lara.ansanelli@usp.br).

P. Alfredini is with the Department of Hydraulics of Universidade de São Paulo, São Paulo, SP 05508-020 Brazil (e-mail: afredin@usp.br).

systems on existing buildings and streets along the coastal areas [3].

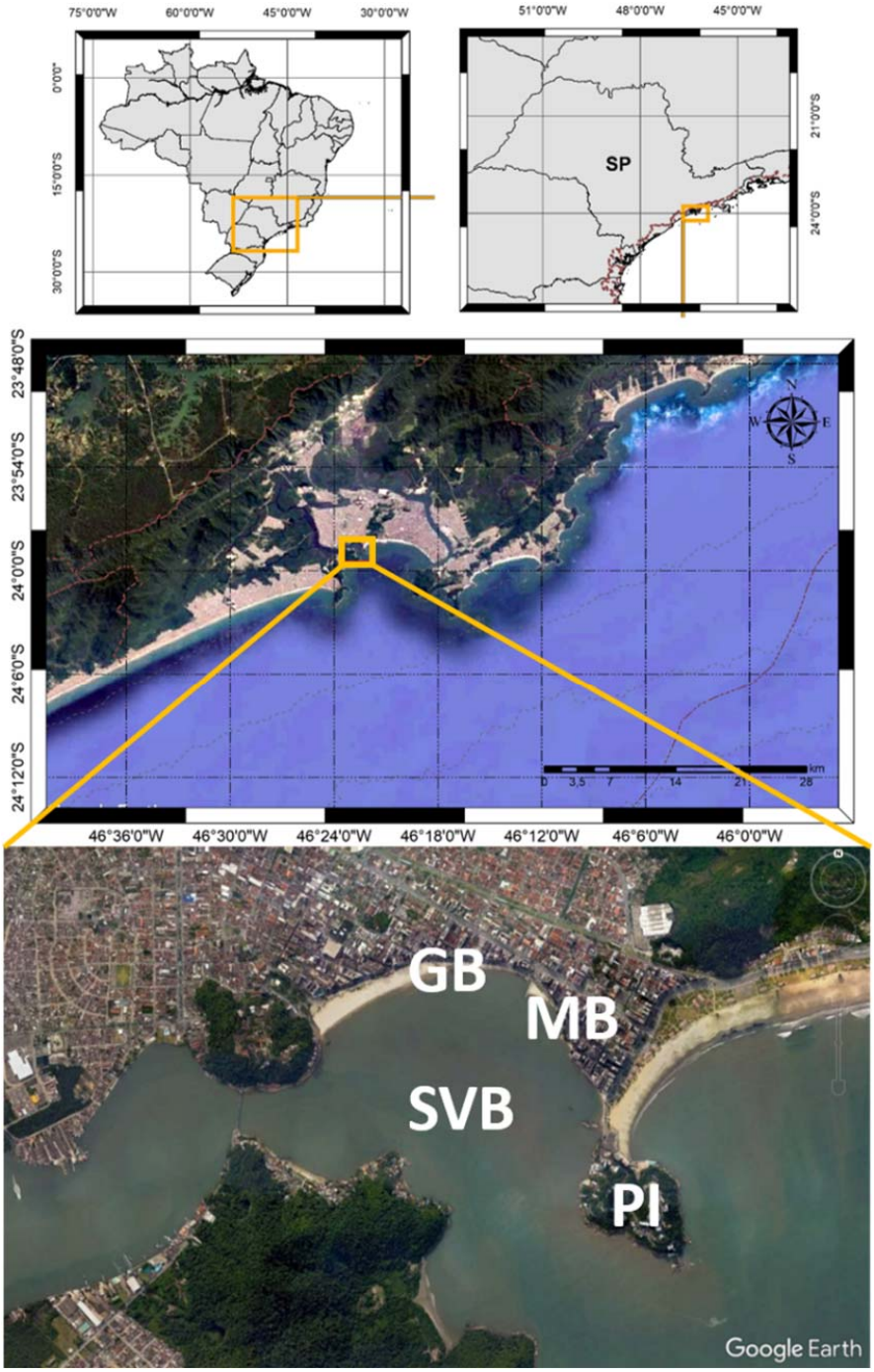

Fig. 1 Location of the study area in Sao Paulo state (SP), in the Brazilian Southeast coast. Inferior Panel: São Vicente Bay (SVB) overview: Porchat Island (PI), Milionários Beach (MB) and Gonzaguinha Beach (GB)

This study aims to evaluate the effectiveness of the two groins as defense structures in terms of the sedimentary dynamics of Gonzaguinha and Milionários Beaches against the waves and the local currents hydrodynamics, as well as to propose additional defense work in the region. For this, a numerical modelling study of the hydrodynamic, wave processes and transport of sediments was conducted.

II. Methodology

A. Numerical Modelling

The Delft3D software was applied for numerical modelling by using the Delft3D-FLOW, Delft3D-WAVE and Delft3D-SED modules [4].

Two numerical grids of different domains and resolutions were created (Fig. 2). Grid 1 was created to represent a larger

domain, covering the external region of São Vicente and Santos Bays. Grid 2 was created for a smaller domain concentrated in São Vicente Bay, with higher resolution in Gonzaguinha and Milionários Beaches. Thus, the hydrodynamical and wave results of Grid 1 were used to downscale large and mesoscale process to the Grid 2 using the off-line grid nesting method.

The depth associated with Grid 1 was obtained by digitizing the bathymetric dimensions from "Diretoria de Hidrografia e Navegação (DHN)" of Brazilian Navy's nautical charts. The depth from Grid 2 was accessed by a synthesis of DHN nautical charts and a field-collected topography at the beaches.

In order to represent the atmospheric field (wind and pressure), map results extracted from the Climate Forecast System Reanalysis version 2 (CFSRv2) [5] were used.

The tidal level was added to a meteorological level to compose a sea surface elevation, inserted as a time series. Tidal harmonic constants obtained from the TPXO Global Tidal Solutions [6], [7] were used to predict tidal sea level. Time-series results were extracted from the CFSRv2 [5] to represent the meteorological level.

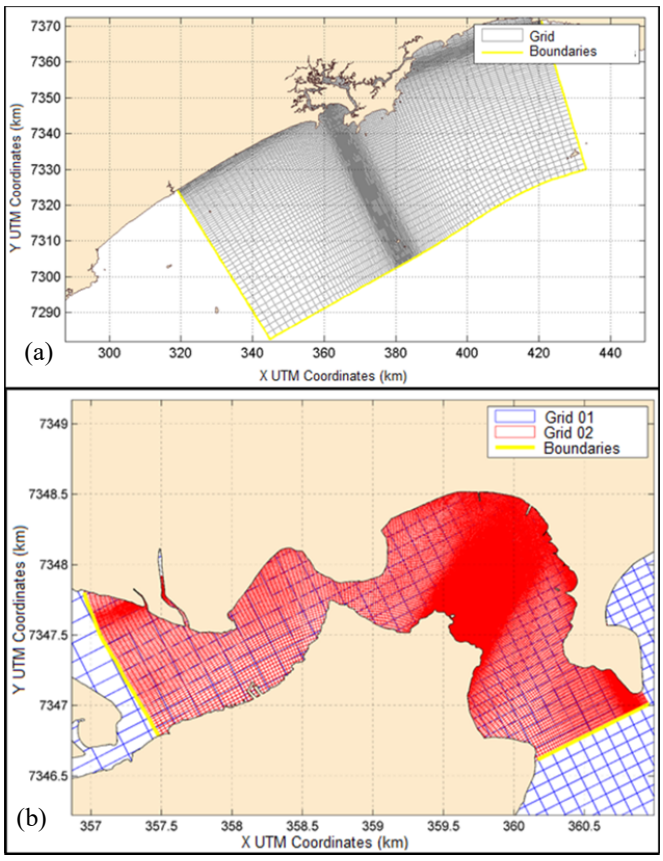

Fig. 2 (a) Grid 1 representing the bigger dominium, (b) Grid 2 representing the smaller dominium with higher resolution

The wave modelling was forced with significant height, direction and peak period from the Wave Watch III (WW3) global model results [8]-[11].

The sediment transport modelling was performed only in Grid 2, with the highest resolution. The features of the sediment map were structured based on [12], which demonstrated that Gonzaguinha and Milionários beaches are formed by a bimodal grain size configuration of fine sand (0.125 mm) and very fine sand (0.063 mm) fractions, with predominance of fine sand nearby the groins. However, only the grain size of 0.125 mm was chosen to be implemented in the numerical modelling of sediment transport since this fraction represents the majority of the sediments in the area of interest (southeastern end of Gonzaguinha Beach).

The calibration procedure consisted of checking the general definitions (i.e. numerical grids, bathymetry, boundary conditions, etc.) and adjusting numerical parameters seeking satisfactory cross-checks between modelled results and measured data. The objective was to apply a model that reliably reproduces the observed processes in the system.

The modelling processes were calibrated with the use of statistical comparisons between their results and recorded data of water level (at 2 geographically different points), current speed (3 points) and wave parameters. The statistical parameters used in the calibration step were the Absolute Mean Error Statistic [13], the R9oot-Mean-Square Error Statistic [13] and the index of agreement [14]. The values obtained for the errors and the index of agreement validate the general configuration of the models and, therefore, were considered as statistically representative of reality.

B. Oceanographic Scenario

The main inducer of short and medium-term coastal processes is the wave system, responsible for the transport in the longitudinal and transversal directions to the coastline [15].

To define the hydrodynamic scenarios operated in sediment modelling, a wave force calculation was executed within the 38-year wave series. The analysis was carried out to determine the synergy [16] between significant height (H) and peak period (T). The equation of synergy is.

$$P = \frac{\rho g^2 H^2 T}{32\pi} \quad (1)$$

Once the wave force was determined for each instant of the time series, a simple statistical analysis was performed to determine the maximum energy values (Fig. 3) of each month, as well as the maximum cumulative energy of each month and each year. The series used is the same series of WW3 adopted at the boundary of the larger wave domain model (Grid 1).

Based on the results, the months from April to September 2010 were selected as they show the highest maximum wave forces within the analyzed period.

Considering the geographical orientation of São Vicente Bay, it is known that the wave directions that mainly reach its interior are those coming from SE, S and SSE quadrants. Fig. 4 shows the joint occurrence of significant height and directions in the period from April to September 2010 for significant height and Fig. 5 shows the corresponding directional histogram.

With the joint analysis of directions occurring in the period, it is concluded that the directions SE, S and SSE correspond to

almost 60% of the waves that reach the region in the considered period.

	January	February	March	April	May	June	July	August	September	October	November	December	Total
1979	3,87E+04	4,71E+04	1,28E+05	1,42E+05	1,32E+05	1,42E+05	1,50E+05	6,40E+04	1,06E+05	1,04E+05	1,78E+05	1,51E+05	1,38E+06
1980	1,56E+05	1,52E+05	1,18E+05	1,05E+05	1,03E+05	1,24E+05	1,49E+05	1,09E+05	1,65E+05	1,00E+05	7,74E+04	5,74E+04	1,42E+06
1981	8,98E+04	7,19E+04	1,12E+05	1,66E+05	1,97E+05	2,70E+05	8,45E+04	9,75E+04	1,76E+05	1,12E+05	3,65E+04	4,44E+04	1,46E+06
1982	8,40E+04	8,10E+04	6,17E+04	1,36E+05	6,29E+04	8,73E+04	1,85E+05	1,13E+05	2,06E+05	1,52E+05	1,20E+05	2,26E+05	1,52E+06
1983	7,73E+04	1,09E+05	8,59E+04	8,93E+04	6,10E+04	7,50E+04	8,67E+04	1,63E+05	1,64E+05	1,01E+05	8,51E+04	6,11E+04	1,16E+06
1984	6,52E+04	1,00E+05	1,02E+05	1,08E+05	7,26E+04	1,07E+05	1,60E+05	1,82E+05	1,35E+05	1,04E+05	1,99E+05	8,48E+04	1,42E+06
1985	9,17E+04	9,68E+04	5,94E+04	4,98E+04	1,24E+05	1,86E+05	1,53E+05	2,06E+05	7,43E+04	1,35E+05	8,38E+04	7,93E+04	1,34E+06
1986	5,26E+04	5,77E+04	7,11E+04	2,09E+05	1,51E+05	9,92E+04	1,41E+05	6,79E+04	1,18E+05	1,17E+05	1,58E+05	8,74E+04	1,33E+06
1987	3,91E+04	1,73E+05	2,79E+05	8,39E+04	1,36E+05	1,17E+05	2,84E+05	1,41E+05	1,16E+05	5,57E+04	5,49E+04	4,69E+04	1,53E+06
1988	5,40E+04	1,04E+05	6,37E+04	1,39E+05	9,01E+04	8,59E+04	1,33E+05	2,32E+05	8,38E+04	5,80E+04	8,62E+04	5,83E+04	1,19E+06
1989	3,62E+04	4,44E+04	9,70E+04	5,15E+04	1,84E+05	8,54E+04	1,47E+05	6,41E+04	1,73E+05	1,22E+05	6,78E+04	8,83E+04	1,16E+06
1990	1,12E+05	7,00E+04	4,37E+04	1,98E+05	1,57E+05	1,79E+05	1,81E+05	1,38E+05	1,16E+05	9,20E+04	1,31E+05	1,09E+05	1,53E+06
1991	6,77E+04	6,26E+04	7,78E+04	1,52E+05	1,08E+05	1,00E+05	1,03E+05	1,38E+05	1,43E+05	1,41E+05	8,44E+04	9,97E+04	1,28E+06
1992	9,00E+04	5,10E+04	1,03E+05	8,85E+04	1,26E+05	1,39E+05	1,21E+05	1,12E+05	9,26E+04	7,81E+04	1,23E+05	5,32E+04	1,18E+06
1993	7,27E+04	9,88E+04	6,90E+04	7,41E+04	1,30E+05	1,34E+05	1,14E+05	1,38E+05	8,31E+04	1,18E+05	6,27E+04	8,62E+04	1,18E+06
1994	5,87E+04	5,71E+04	1,36E+05	2,16E+05	1,31E+05	1,53E+05	1,70E+05	7,49E+04	1,22E+05	1,86E+05	1,40E+05	1,04E+05	1,55E+06
1995	6,16E+04	1,20E+05	5,00E+04	1,56E+05	1,31E+05	7,46E+04	7,31E+04	1,41E+05	2,39E+05	1,36E+05	1,28E+05	8,65E+04	1,40E+06
1996	4,43E+04	1,30E+05	6,40E+04	1,29E+05	1,21E+05	1,45E+05	2,68E+05	6,78E+04	7,65E+04	1,15E+05	6,25E+04	3,51E+04	1,26E+06
1997	4,80E+04	9,01E+04	5,91E+04	1,15E+05	1,44E+05	1,74E+05	9,92E+04	1,70E+05	1,00E+05	1,74E+05	8,58E+04	6,51E+04	1,33E+06
1998	7,64E+04	9,33E+04	1,17E+05	1,28E+05	1,16E+05	1,63E+05	1,48E+05	1,38E+05	1,43E+05	8,56E+04	9,64E+04	8,06E+04	1,38E+06
1999	5,29E+04	7,52E+04	7,76E+04	1,44E+05	2,46E+05	1,33E+05	1,29E+05	2,24E+05	1,40E+05	8,77E+04	7,95E+04	5,77E+04	1,45E+06
2000	5,47E+04	7,97E+04	5,26E+04	7,56E+04	1,13E+05	8,59E+04	1,81E+05	1,32E+05	8,62E+04	6,44E+04	1,01E+05	1,09E+05	1,13E+06
2001	4,60E+04	7,02E+04	5,78E+04	5,33E+04	2,12E+05	1,10E+05	9,79E+04	9,22E+04	1,29E+05	1,03E+05	5,49E+04	7,57E+04	1,10E+06
2002	1,44E+05	1,46E+05	1,80E+05	7,72E+04	1,05E+05	1,04E+05	9,66E+04	1,03E+05	1,56E+05	1,31E+05	8,67E+04	6,18E+04	1,39E+06
2003	8,13E+04	3,86E+04	8,76E+04	1,30E+05	1,28E+05	1,13E+05	9,73E+04	1,14E+05	1,49E+05	4,64E+04	1,44E+05	8,66E+04	1,22E+06
2004	5,69E+04	3,41E+04	6,60E+04	7,92E+04	1,29E+05	9,06E+04	1,26E+05	1,06E+05	1,84E+05	9,72E+04	1,36E+05	7,78E+04	1,18E+06
2005	6,38E+04	6,91E+04	8,66E+04	1,48E+05	1,40E+05	1,11E+05	1,46E+05	1,42E+05	1,14E+05	1,08E+05	7,51E+04	6,89E+04	1,27E+06
2006	5,92E+04	5,77E+04	9,55E+04	1,51E+05	9,14E+04	2,14E+05	1,79E+05	2,00E+05	2,07E+05	1,33E+05	1,41E+05	6,05E+04	1,59E+06
2007	1,15E+05	6,75E+04	3,84E+04	1,65E+05	1,63E+05	1,54E+05	2,67E+05	1,10E+05	1,38E+05	7,36E+04	1,20E+05	9,64E+04	1,51E+06
2008	5,44E+04	5,69E+04	8,16E+04	1,02E+05	1,38E+05	1,54E+05	8,62E+04	9,61E+04	1,31E+05	1,23E+05	1,56E+05	1,09E+05	1,29E+06
2009	1,27E+05	6,66E+04	4,95E+04	1,75E+05	1,40E+05	9,52E+04	2,48E+05	1,18E+05	1,04E+05	1,04E+05	4,33E+04	1,31E+05	1,40E+06
2010	6,31E+04	1,77E+05	1,31E+05	3,31E+05	1,09E+05	1,81E+05	1,46E+05	1,89E+05	1,52E+05	1,24E+05	1,07E+05	2,08E+05	1,92E+06
2011	6,63E+04	6,55E+04	1,35E+05	6,89E+04	2,59E+05	2,41E+05	1,46E+05	2,27E+05	1,13E+05	6,93E+04	5,16E+04	1,19E+05	1,56E+06
2012	4,63E+04	5,76E+04	1,07E+05	1,32E+05	1,18E+05	1,57E+05	2,04E+05	1,04E+05	1,86E+05	9,49E+04	8,40E+04	7,25E+04	1,36E+06
2013	1,29E+05	6,51E+04	1,14E+05	1,84E+05	1,26E+05	1,03E+05	1,80E+05	1,58E+05	1,94E+05	1,58E+05	1,31E+05	1,92E+05	1,74E+06
2014	1,08E+05	1,31E+05	6,75E+04	1,36E+05	1,57E+05	2,25E+05	1,08E+05	1,57E+05	1,14E+05	7,47E+04	7,35E+04	7,40E+04	1,42E+06
2015	7,60E+04	9,32E+04	9,73E+04	1,08E+05	1,35E+05	1,84E+05	1,39E+05	8,92E+04	1,41E+05	9,65E+04	1,13E+05	5,52E+04	1,33E+06
2016	5,16E+04	4,59E+04	4,47E+04	1,43E+05	6,23E+04	1,75E+05	1,07E+05	1,75E+05	1,11E+05	2,16E+05	8,65E+04	1,21E+05	1,34E+06
Total	2,81E+06	3,21E+06	3,47E+06	4,94E+06	5,05E+06	5,27E+06	5,63E+06	5,09E+06	5,18E+06	4,19E+06	3,85E+06	3,48E+06	

Fig. 3 Maximum wave forces for each month from 1979 to 2016

Height(m)	N	NNE	NE	ENE	E	ESE	SE	SSE	S	SSW	SW	WSW	W	WNW	NW	NNW	Total
0.00-0.50	0	0	0	0	0	0	0	0	0	0	0	0	0	0	0	0	0
0.50-1.00	0	0	0	0	2,34	1,4	0,12	0,88	0,29	0	0	0	0	0	0	0	5,02
1.00-1.50	0	0	0	0	9,52	5,2	3,15	3,68	6,37	0,88	0	0	0,06	0,12	0	0	28,97
1.50-2.00	0	0	0	0,35	6,07	1,75	4,96	4,38	4,73	1,17	0,12	0,12	0,06	0	0	0	23,71
2.00-2.50	0	0	0	0,35	2,98	0,93	5,02	2,86	6,02	1,52	0,23	0	0	0	0	0	19,92
2.50-3.00	0	0	0	0	0,82	1,05	2,34	2,34	4,26	0,58	0,23	0	0	0	0	0	11,62
3.00-3.50	0	0	0	0	0	0,53	1,05	0,99	2,75	0,93	0,12	0	0	0	0	0	6,37
3.50-4.00	0	0	0	0	0	0,53	0,23	0	1,46	0,47	0	0	0	0	0	0	2,69
4.00-4.50	0	0	0	0	0	0,29	0,41	0,06	0,06	0,18	0	0	0	0	0	0	0,99
4.50-5.00	0	0	0	0	0	0	0,29	0,23	0	0	0	0	0	0	0	0	0,53
5.00-5.50	0	0	0	0	0	0	0,18	0	0	0	0	0	0	0	0	0	0,18
Total	0	0	0	0,7	21,73	11,68	17,76	15,42	25,93	5,72	0,7	0,12	0,12	0,12	0	0	
Average Height	0	0	0	2,07	1,53	1,74	2,18	1,96	2,17	2,34	2,45	1,72	1,38	1,23	0	0	
Maximum Height	0	0	0	2,48	2,85	4,07	5,18	4,66	4,13	4,29	3,26	1,94	1,64	1,31	0	0	

Fig. 4 Diagram of joint occurrence of the significant height (m) of waves resulting from WW3 between April and October 2010

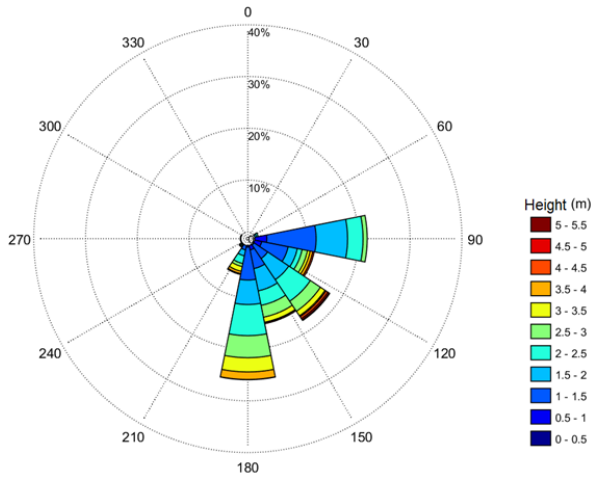

Fig. 5 Wind rose of significant height for the period from April to September 2010.

C. Engineering Scenarios

Coastal defense and stabilization works are used to maintain or reconstruct beaches, or to protect buildings and existing infrastructure on the shoreline.

Once the models are calibrated and the oceanographic scenario was defined, the simulations for the engineering scenarios were tested. The first tested scenario, Engineering Scenario 1 (ES1), represents the configuration of the existing structures with two groins (Fig. 6). The modelling with this scenario was carried out to analyze the effectiveness of the existing structures on the sedimentary processes involved in the region.

Once the sedimentary balance was characterized by a significant sand deficit in the supply of a large stretch of the beach, the Engineering Scenario 2 (ES2; Fig. 7) was implemented as a design of breakwater structures (parallel to the coast) coupled to the groins, seeking to evaluate this scenario as an alternative of rigid works of coastal protection to the erosive action of waves.

TABLE I
FEATURES OF ENGINEERING SCENARIO 2 (ES2)

	Length (m)	Lb/Y
T1: Groin 1 and Breakwater 1	70	1
T2: Groin 2 and Breakwater 2	90	1

Reference [17] recommends breakwater structures to be designed so that they form protrusions on their back. The distance between the structure and the coastline (Y), the length of the breakwater and the spacing between segments of the breakwater determine the features formed on the coastline.

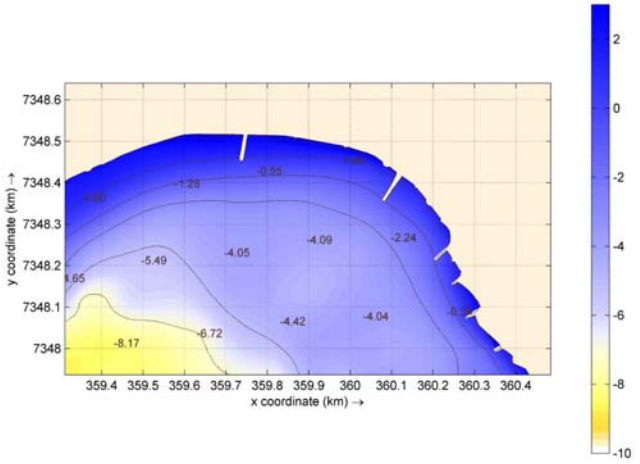

Fig. 6 Engineering works scenario 1 (ES1) within the current study area configuration. The bathymetry is represented by the lateral colour scale

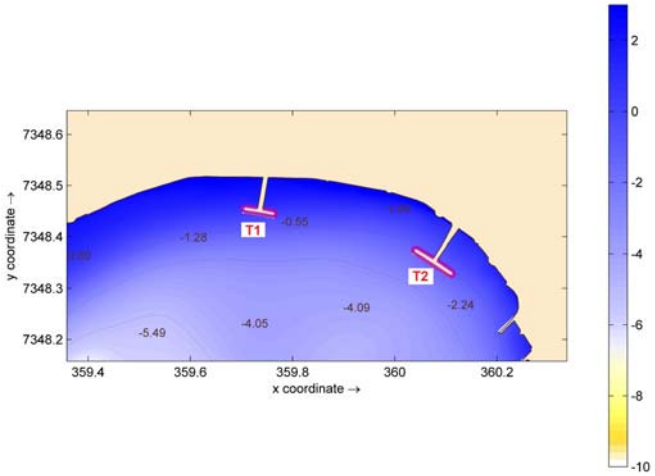

Fig. 7 Engineering works scenario 2 (ES2), with the implementation of breakwaters accomplished. The bathymetry is represented by the lateral colour scale

In [17], several relations are presented between the parameters length of the breakwaters (Lb) and the distance from the project beach to the breakwater (Y), obtained in different studies, and the formation of tombolos or protrusions on the coast. In general, the ratio for the formation of protrusions should be $Lb / Y \leq 1$.

In the present study, ES2 was used to verify the feasibility of using the pre-existing structures (groins) to couple the breakwaters, therefore, they are not breakwaters detached from the coast, but structures in the shape of "T" (T1 and T2; Fig. 7). The length of each breakwater (Lb) was designed with the same length as the corresponding groin (Y), as described in Table I.

III. Results and Discussion

The results presented are illustrations of the beach responses obtained from simulations with real hydrodynamic conditions and indicate the effect of a period of high wave energy on morphology, as well as the effect of the structure on the circulation and local sediment transport. It is noteworthy that, although the images show a scale of sedimentation, the results have a qualitative aspect and are interpreted in terms of areas of sedimentation and erosion. The following results are from Grid 2.

A. Beach Profiles

Fig. 8 shows the position and extent of the beach profiles analyzed in this section. The behaviour of the profiles in the same position was analyzed considering the initial moment and the results of each scenario, for the period from April to September 2010 in terms of bathymetric gain or loss.

The profiles are presented in a way that the distance 0 represents the point on the beach and the increase in distance is projected towards the center of the Bay.

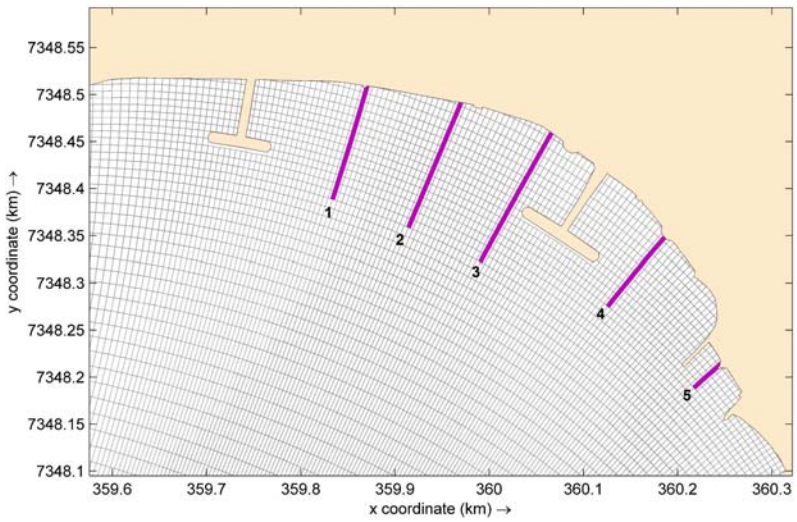

Fig. 8 Position of beach profiles

Profile 1 (Fig. 9 (a)) shows, both in ES1 and ES2, topography losses at 40 meters from the beach, with the lost volume being sedimented after 60 meters, thus revealing a tendency of transport to the opposite direction of the beach.

Profile 2 (Fig. 9 (b)) shows a more accentuated topographic change for ES1 compared to ES2.

Profile 3 (Fig. 9 (c)) presents a behaviour similar to profile 2, with lower sediment losses in the locations closest to the beach for ES2, which has the support of coupled breakwater structures.

Profile 4 (Fig. 9 (d)) shows sediment loss, with a decrease in topography in ES1. However, it presented a sedimentary increase with the presence of the works of ES2, with gains of approximately 50 cm in a horizontal extension of 40 meters.

Profile 5 (Fig. 9 (e)), located in a portion where the strip of emersed sand is narrow, presented a loss of topography from 10 meters away from the beach in both engineering scenarios addressed, with the lost volume being sedimented after 25 meters, revealing, therefore, a trend of transport in the opposite direction of the beach.

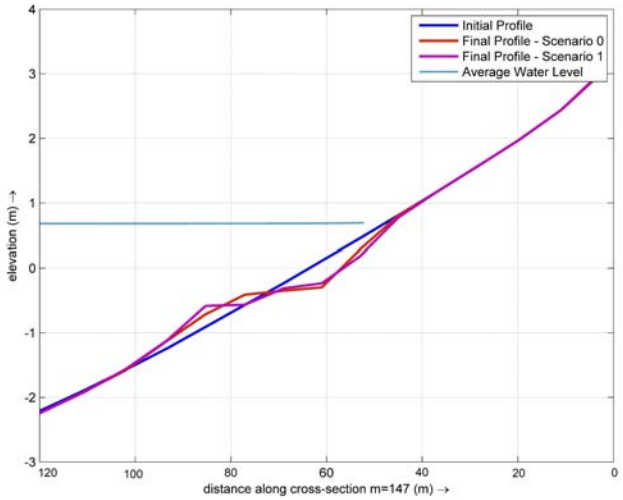

(a)

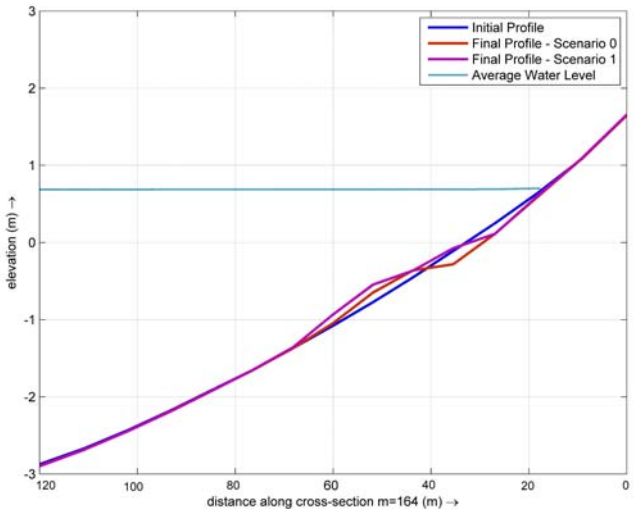

(b)

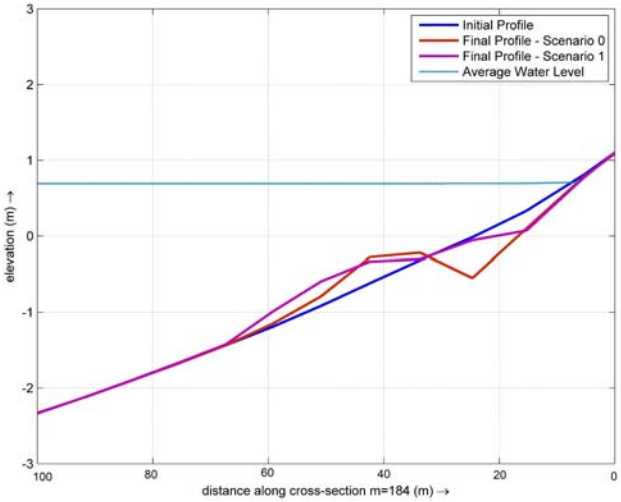

(c)

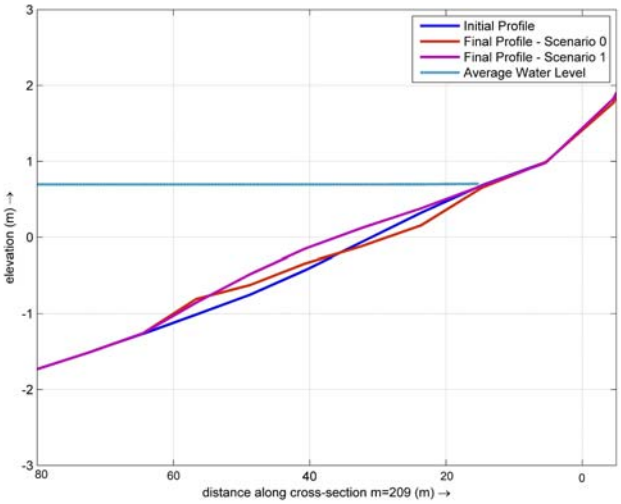

(d)

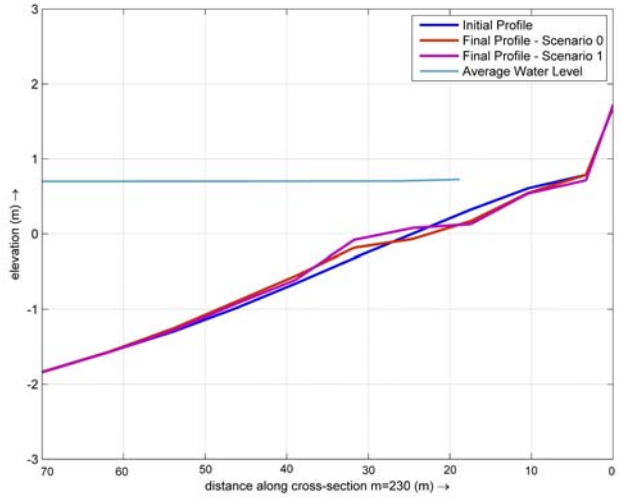

(e)

Fig. 9 Beach Profile 1 (a), 2 (b), 3 (c), 4 (d) and 5 (e) for Beach Initial Profile (dark blue), Final Profile for ES1 (red), Final Profile for ES2 (pink) and Average Water Level (green)

All the profiles analyzed showed erosive tendencies for the period simulated with ES1. The ES2, with coupled breakwaters, shows lower losses in all the profiles analyzed in comparison to ES1, even in profiles not adjacent to the coupled structure. Profile 4, in ES2, demonstrated deposition of sediment between the distances of 20 and 60 m.

B. Sediment Transport

Residual currents represent the average flow for the analyzed period. The estimation of the spatial distribution of the intensities and predominant directions of currents was performed for the entire domain and resolution of Grid 2 and for the period defined in the ocean scenario.

The study of residual currents has always been related to studies of long-term transport processes such as dispersion of pollutant discharge, phytoplankton blooms and sediment dynamics [18]. In both scenarios, the results indicate that the direction of residual sediment transport has a general direction from East to West in the interior of São Vicente Bay (Figs. 10 and 11). The sediment is then retained on the groins and at the foot of the Morro do Barbosa (western end of Gonzaguinha), which is the point where the beach arch ends.

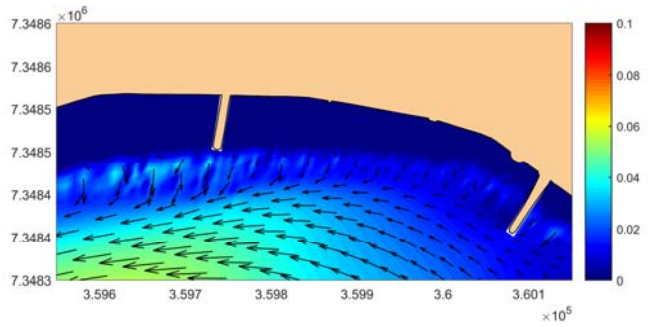

Fig. 10 Residual current for ES1

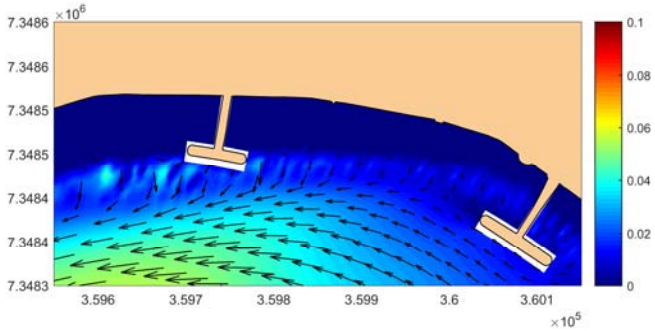

Fig. 11 Residual current for ES2

It was observed over the years [3], [19] and by the ES1 simulation of this study that the beach around the groins was not recovered and that it presents erosive tendencies. The deposition and erosion regime represented on the maps also shows a transport behaviour dominated by incident waves, mainly those of high energy and with SE, S and SSE directions, due to the presence of currents in the normal direction closer to the beach (Figs. 10 and 11). The behaviour of the normal currents results in the pattern observed in Figs. 12 and 13 showing erosion adjacent to the coastline with deposition towards the center in the Bay.

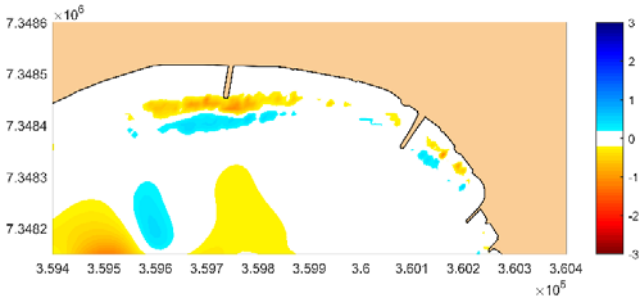

Fig. 12 Cumulative erosion (hot colours) and deposition (cold colours) for ES1

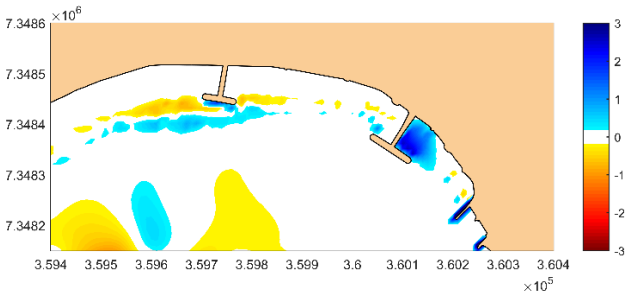

Fig. 13 Cumulative erosion (hot colours) and deposition (cold colours) for ES2

Figs. 14 and 15 show the general retreat of the coastlines when submitted to extreme events (high wave energy), showing only progradation in the back to the SE of the T2 structure (Figs. 15 and 16), which was configured as a "zone of shade" for the incidence of waves and is favoured by the direction of the coastal drift.

It is important to note that the landfill works associated with the artificial closure of the Porchat Island's channel, as mentioned in the introduction session of this study, are the most likely causes of the lack of sediment input for these beaches. As the coastal drift of the adjacent outer stretch of these beaches (Praia de Itararé) is predominantly to the west, the interruption of sediment caused by the establishment of the tombolo made the Milionários beach and the southeastern end of Gozaguinha start to suffer erosion [3].

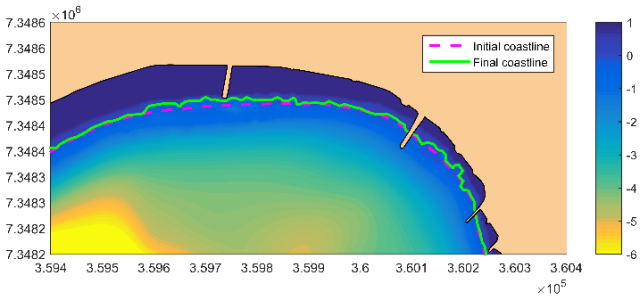

Fig. 14 Final morphology and initial (dotted pink) and final (green) coastline for ES1

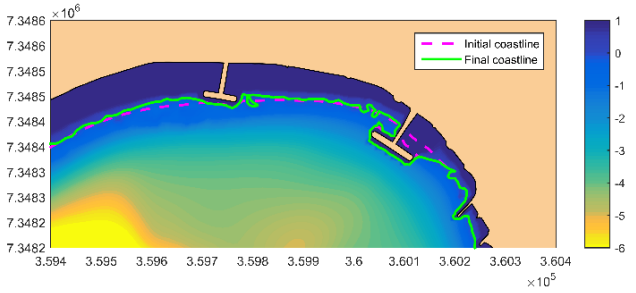

Fig. 15 Final morphology and initial (dotted pink) and final (green) coastline for ES2

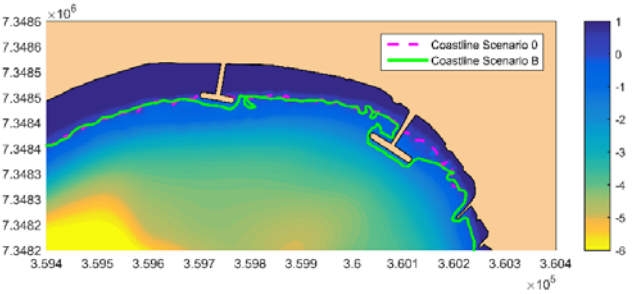

Fig. 16 Final morphology of ES2 and final coastlines for ES1 (dashed pink) and ES2 (green)

IV. Conclusions

This study presents results of numerical simulations of the sedimentary behaviour of Milionários and Gonzaguinha beaches, located in the interior of São Vicente Bay. It has been considered the scenario of existing works in the region (2 groins) and a second scenario with the breakwaters coupled at the end of each groin, forming structures in "T" shape.

The presence of the coupled breakwaters attenuated the sedimentary losses; however, they do not prevent the erosion process of the places not directly protected by the structure. This statement is confirmed by the analysis of the maps of the coastline and cumulative sedimentation and erosion, showing that the depositions were significant at the back of the southeastern segment of T2, helping in the recovery of the sand strip in this region. It is also possible to affirm that the normal transport to the coastline indicated strong action of the incident waves of S, SE and SSE in this period, removing sediments from the beach and depositing in deeper places.

Further design and simulation of additional engineering scenarios are needed including detached breakwaters, artificial feeding of regions that are in a deficit of sand or even considering the reopening of the Porchat Island channel.

References

[1] L. C. Van Rijn, J. S. Ribberink, J. Van Der Werf, & D. J. Walstra. Coastal sediment dynamics: recent advances and future research needs. Journal of hydraulic research, 51(5), 475-493. 2013.

[2] P. Alfredini, A. Pezzoli, E. Arasaki, "Impact of climate changes on the Santos Harbor, São Paulo State (Brazil)". TransNav, the International Journal on Marine Navigation and Safety of Sea Transportation, v. 7, n. 4, 2013, pp. 609–617.

[3] A. Farinaccio; G. S. V. Cazolli; M.G. Tessler. "Variações da linha de costa nas baías de Santos e São Vicente". Quaternary and Environmental Geosciences, v.1, 2009, pp. 42-48.

[4] Deltares. User Manual Delft3D-FLOW. Simulation of Multi-Dimensional Hydrodynamic and Transport Phenomena, Including Sediments. Deltares, Delft, The Netherlands. 2018, pp. 702-704.

[5] Saha et al. The NCEP Climate Forecast System Version 2. Journal of Climate, 27, 2185–2208. doi: http://dx.doi.org/10.1175/JCLI-D-12-00823.1. 2014.

[6] G. D. Egbert, A. F. Bennett, M. G. Foreman. TOPEX/POSEIDON tides estimated using a global inverse model. Journal of Geophysical Research: Oceans, v. 99, n. C12, 1994, pp. 24821-24852.

[7] G. D. Egbert, S. Y. Erofeeva. "Efficient inverse modeling of barotropic ocean tides". Journal of Atmospheric and Oceanic Technology, v. 19, n. 2, 2002, pp. 183-204.

[8] H.L. Tolman. User manual and system documentation of WAVEWATCH-III version 1.15. NOAA/NWS/NCEP/OMB Technical Note 151, 1997, pp 97.

[9] H.L. Tolman. User manual and system documentation of WAVEWATCH-III version 1.18. NOAA/NWS/NCEP/OMB Technical Note 166, 1999, pp 110.

[10] H.L. Tolman. User manual and system documentation of WAVEWATCH-III version 2.22. NOAA/NWS/NCEP/MMAB Tech. Note 222, 2002, pp. 133.

[11] H.L. Tolman. User manual and system documentation of WAVEWATCH-III version 3.14. NOAA/NWS/NCEP/OMB Technical Note 276, 2009, 194 pp, + Appendices.

[12] V.A.P. Alexandre. "Análise morfodinâmica das praias arenosas de São Vicente/SP". Bachelor Thesis. Universidade de Mont Serrat. 2010.

[13] C.J. Willmott. "Some comments on the evaluation of model performance". American Meteorological Society Bulletin, 1982, pp. 1309-1313.

[14] J. Willmott, D. E. Wicks. "An Empirical Method for the Spatial Interpolation of Monthly Precipitation within California", Physical Geography, 1:1,59-73, DOI:10.1080/02723646.1980.10642189. 1980.

[15] D.H. Muehe. Erosão e Progradação do Litoral Brasileiro. Brasília, Ministério Meio Ambiente, 2006, pp. 476-478.

[16] C. Pianca, P.L.F. Mazzini, E. Siegle. Brazilian offshore wave climate based on WW3 reanalysis. Braz. J. Oceanogr., 2010, pp. 53–70.

[17] US Army Corps of Engineer, Shore Protection Projects. In: Coastal Engineering Manual, 2002, Cap. 3. p. 2-4.

[18] P. Cugier; P Le Hir. "Development of a 3D Hydrodynamic Model for Coastal Ecosystem Modelling. Application to the Plume of the Seine River (France)". Estuarine, Coastal and Shelf Science, Elsevier Science, 2002.

[19] C.R.G. Souza, F.O. Barbosa. "Taxas de Recuo da Praia do Gonzaguinha (São Vicente-SP) no Período de 1962 a 2001, baseadas em Fotografias Aéreas. Belém, PA". In: XI Congresso da Associação Brasileira de Estudos do Quaternário – ABEQUA, Belém, PA, 4 a 11 de novembro de 2007. Anais, CD-ROM. 2007.